

# DNA methyltransferases contribute to the fungal development, stress tolerance and virulence of the entomopathogenic fungus *Metarhizium robertsii*

Yulong Wang<sup>1</sup> · Tiantian Wang<sup>1</sup> · Lintao Qiao<sup>1</sup> · Jianyu Zhu<sup>1</sup> · Jinrui Fan<sup>1</sup> ·  
Tingting Zhang<sup>1</sup> · Zhang-xun Wang<sup>1,2</sup> · Wanzhen Li<sup>1,3</sup> · Anhui Chen<sup>1,4</sup> · Bo Huang<sup>1</sup>

Received: 10 October 2016 / Revised: 4 February 2017 / Accepted: 11 February 2017 / Published online: 25 February 2017  
© Springer-Verlag Berlin Heidelberg 2017

**Abstract** DNA methylation is an important epigenetic mark in mammals, plants, and fungi and depends on multiple genetic pathways involving de novo and maintenance DNA methyltransferases (DNMTases). *Metarhizium robertsii*, a model system for investigating insect-fungus interactions, has been used as an environmentally friendly alternative to chemical insecticides. However, little is known concerning the molecular basis for DNA methylation. Here, we report on the roles of two DNMTases (MrRID and MrDIM-2) by characterizing  $\Delta MrRID$ ,  $\Delta MrDIM-2$ , and  $\Delta RID/\Delta DIM-2$  mutants. The results showed that approximately 71, 10, and 8% of <sup>13</sup>C sites remained in the  $\Delta MrRID$ ,  $\Delta MrDIM-2$ , and  $\Delta RID/\Delta DIM-2$  strains, respectively, compared with the wild-type (WT) strain. Further analysis showed that MrRID regulates the specificity of DNA methylation and MrDIM-2 is responsible for most DNA methylation, implying an interaction or cooperation between MrRID and MrDIM-2 for DNA methylation. Moreover, the  $\Delta MrDIM-2$  and  $\Delta RID/\Delta DIM-2$  strains showed more defects in radial growth and conidial

production compared to the WT. Under ultraviolet (UV) irradiation or heat stress, an obvious reduction in spore viability was observed for all the mutant strains compared to the WT. The spore median lethal times (LT<sub>50</sub>s) for the  $\Delta MrDIM-2$  and  $\Delta RID/\Delta DIM-2$  strains in the greater wax moth, *Galleria mellonella*, were decreased by 47.7 and 65.9%, respectively, which showed that MrDIM-2 is required for full fungal virulence. Our data advances the understanding of the function of DNMTase in entomopathogenic fungi, which should contribute to future epigenetic investigations in fungi.

**Keywords** *Metarhizium robertsii* · DNA methyltransferase · DNA methylation · Phenotype · Virulence

## Introduction

In eukaryotes, DNA methylation describes the transfer of a methyl group (CH<sub>3</sub>) to the fifth position of a cytosine residue and occurs almost exclusively in association with transposable elements and repeat sequences (Jeon et al. 2015; Suzuki and Bird 2008). In the nucleus, cytosine methylation cooperates with N-terminal histone modifications to establish a silenced chromatin structure, thus regulating nuclear gene expression (Shock et al. 2011). Methylation patterns in animals are established by two de novo DNA methyltransferases (DNMTases), DNMTase 3a (DNMT3a) and DNMTase 3b (DNMT3b), and are maintained by DNMTase 1 (DNMT1). In plants, domains that are rearranged by methyltransferase 2 (DRM2) establish the DNA methylation pattern maintained by methyltransferase 1 (MET1) and chromo-methylase 3 (CMT3) (Cao and Jacobsen 2002; Law and Jacobsen 2010; Li 2002). These genes function within an ancient regulatory mechanism shared by eukaryotes, serving in diverse roles often related to the repression of gene expression (Feng et al.

**Electronic supplementary material** The online version of this article (doi:10.1007/s00253-017-8197-5) contains supplementary material, which is available to authorized users.

✉ Bo Huang  
bhuang@ahau.edu.cn

- <sup>1</sup> Anhui Provincial Key Laboratory of Microbial Pest Control, Anhui Agricultural University, Hefei 230036, China
- <sup>2</sup> School of Plant Protection, Anhui Agricultural University, Hefei 230036, China
- <sup>3</sup> Engineering Technology Research Center of Microbial Fermentation Anhui Province, Anhui Polytechnic University, Wuhu 241000, China
- <sup>4</sup> Department of Food and Biology, Xuzhou Institute of Technology, Xuzhou 221008, China

2010; Jurkowski and Jeltsch 2011; Nanty et al. 2011; Zemach et al. 2010).

The DNMTases in fungi such as *Neurospora crassa*, *Ascoibolus immerses*, and *Magnaporthe oryzae* have been characterized. The methylation mechanism of DNMTases in *N. crassa* has been well studied. Repeat-induced point (RIP) defective (RID) is essential for RIP mutation, and DIM-2 is responsible for all known cytosine methylation events; mutation of either of these DNMTases causes no obvious defect in the phenotype (Freitag et al. 2002; Kouzminova and Selker 2001). In *M. oryzae*, DIM-2 is responsible for DNA methylation and RID regulates the methylation specificity of the genome. Abnormalities in colony morphology, radial growth, and sporulation have been observed in a mutant with a deletion of the *DIM-2* gene (Jeon et al. 2015). In *A. immersus*, the *Masc1* mutation has no obvious defect in the phenotype during vegetative growth but blocks the methylation that is induced premeiotically (methylation induced premeiotically (MIP)) and confers sterility in *Masc1* homozygous dikaryons (Selker 1997).

Most fungi have low levels of DNA methylation, ranging from imperceptible to barely detectable (Liu et al. 2012; Martienssen and Colot 2001; Selker et al. 2003). Approximately 1.5% of cytosines are methylated in the genome of *N. crassa*, while <0.1% of methylcytosines were found to be methylated in *Schizosaccharomyces pombe* and *Aspergillus nidulans* (Antequera et al. 1984; Foss et al. 1993; Selker and Stevens 1987). The variation in genome methylation levels suggests that DNA methylation is not strictly conserved among different fungal species. In *N. crassa* and *Candida albicans*, DNA methylation silences transposable elements and repetitive DNA sequences as a genome defense mechanism (Mishra et al. 2011; Selker et al. 2003). However, DNA methylation plays a role in fungal development throughout the asexual life cycle of *M. oryzae* (Jeon et al. 2015).

*Metarhizium robertsii*, an arthropod pathogen, saprophyte, and beneficial colonizer of rhizospheres, has been used as an environmentally friendly alternative to chemical insecticides (Gao et al. 2011; Roberts and St Leger 2004). *M. robertsii* is also well suited for use as a representative species for simultaneously studying several major lifestyles, including parasitism, saprophytism, and symbiotism, in a way that is not matched by the “model” fungi *Saccharomyces cerevisiae* and *N. crassa* (Bidochka et al. 2001; Fang and St Leger 2010). Despite the considerable progress that has been made with regards to unraveling and understanding the genetic pathways that govern morphogenesis and pathogenicity, there have been no surveys of the impact of DNMTases on important economic characteristics such as conidiation, stress tolerance, or virulence in entomopathogenic fungi (Aramayo and Selker 2013; Wang and St Leger 2014).

To investigate DNMTases in *M. robertsii*, we selected two putative DNMTases, MrRID (accession no. EFZ01240.1) and

MrDIM-2 (accession no. EFZ00016.1), by performing a BLAST search using the amino acid sequences of known DNMTases as queries. Genetic manipulation and traditional bisulfite sequencing (BS-PCR) were used to understand the mechanism of DNMTase on DNA methylation. We further investigated whether disrupting DNMTases impacted the *M. robertsii* life cycle by examining any phenotypic changes in the mutants. Our data suggests a wider role for DNMTases in DNA methylation and the development of entomopathogenic fungi, which should contribute to future epigenetic investigations in fungi.

## Materials and methods

### Fungal strains and growth conditions

The wild-type (WT) *M. robertsii* strain ARSEF 23 (ATCC no. MYA-3075) was generously provided by Dr. Chengshu Wang (Gao et al. 2011). Stock cultures were grown on potato dextrose agar (PDA; 20% potato, 2% dextrose, and 2% agar, w/v) in the dark at 28 °C for 12 days to obtain conidia. Conidia were harvested in a 0.05% Tween 80 aqueous solution, and the conidial suspension was filtered through sterile non-woven fabric to remove mycelia, which were then washed in sterilized water. The final spore concentrations were determined by direct counting using a hemocytometer. Unless otherwise noted, for phenotypic assays, conidial suspensions (1- $\mu$ l suspension,  $1 \times 10^6$  conidia  $\text{ml}^{-1}$ ) of each strain were spotted onto various media.

### Genetic manipulation and fungal transformation

The binary vectors pDHt-SK-bar (conferring resistance against ammonium glufosinate) and pDHt-SK-ben (conferring resistance against benomyl) and the *Agrobacterium* strain AGL-1 were kindly provided by Dr. Chengshu Wang (Gao et al. 2013). Target genes were deleted using an *Agrobacterium*-mediated transformation method as described previously (Duan et al. 2013). In brief, the 5' and 3' flanking regions of *MrRID* and *MrDIM-2* were amplified using WT genomic DNA as a template and the forward and reverse primer pairs *MrRID* 5' flanking, *MrRID* 3' flanking, *MrDIM-2* 5' flanking, and *MrDIM-2* 3' flanking, respectively (Table 1). To construct the *MrRID* deletion vector, the products of the 5' flanking regions were digested with *Xho*I and *Bam*HI (TaKaRa, Dalian, China), while the products of the 3' flanking regions were digested with *Spe*I and *Xba*I (TaKaRa, Dalian, China) and then inserted into the corresponding sites of the binary vector pDHt-SK-bar to produce the binary vector pbar-RID (Fig. 1a). To construct the *MrDIM-2* deletion structure, the 5' and 3' flanking region products were digested with *Pst*I and *Spe*I (TaKaRa, Dalian, China), respectively, and then

**Table 1** PCR primers used in this study

ID <sup>a</sup>	Forward primer (5'-3')	Reverse primer (5'-3')
Primers were designed for disruption and complementation of MrRID and MrDIM-2		
MrRID 5' flanking	CCGCTCGAGAAAGGTGTTTCGCAGTGTTCAGG	CGGGATCCCACAGCGAGTTGAACCAAATGAG
MrRID 3' flanking	GACTAGTAGAGCTGTTGCTGCCTGCCTACT	GCTCTAGACATCTGAATTTCTGCCGCTTTC
MrDIM-2 5' flanking	AACTGCAGTATGAGATTACGATTTTCATGGGT	AACTGCAGTAGTCGATAAAGCTGTGGTAGAT
MrDIM-2 3' flanking	GACTAGTTGCCACATTACTGGTGTGCTCT	GACTAGTGTAAGGACTGCTTGTGGAGACG
MrRID (i, j)	AACTGCAGTTGAGTAAAGGTGTTTCGCAGTG	AACTGCAGAAGTAGGCAGGCAGCAACAG
MrDIM-2 (k, l)	CGGGATCCGGGCAGACTCGACGGGAGTA	CGGGATCCCAGATTCCCAGCCCAAGGTC
Primers were designed for the validation of mutants		
MrRID (a, b)	CAAGCGTCACATTGAACAGTCG	AAGTATTGGCAGGGCGGAGA
MrDIM-2 (g, h)	TTTTCAAAGGGAGGCATTTAGCG	GGTGGTCAGGGAAGGCGATG
bar (c, d)	TCGTCAACCACTACATCGAGAC	GTTTCTGGCAGCTGGACTTC
ben (e, f)	GGTAACTCCACCGCCATCCA	GCAGGGTATTGCCTTTGGACTT
GADPH	CCAGAACATCATTTCCAGCAGCAC	AATGTAGGCAAGGAGATCGAGGACA
MrRID (Southern blotting, p1)	ATGTCTCCGCCCTGCCAATA	ATCACCACATCCTCCGCCTC
MrDIM-2 (Southern blotting, p2)	GAGCAACAATGGACAAGGCAAGA	AAAGAGTGTGAGAAGGGCGGTAG
Primers were designed for traditional bisulfite sequencing		
Scf_009:1,126,800–1,127,100	GCTCGTCAGCGGCATCACAAAT	GCTGTTTGTGGAGGGTATGATGAGTA
Scf_042:35,000–35,449	GCGTCGAATCACAAAGAGTACAGT	ATCATCTACAAACAGCGAGGCA
Scf_009:358,600–359,049	TAAACCCCAAGAATCAAGAAACG	CGCAGGATGGAAGAAGGTAGT
Scf_001:1,427,050–1,427,399	GCAAATCCGCTGGGTCATCCT	CAAAGCGGGCAGACGAAGGT
Scf_001:5,119,700–5,120,149	CTTATGCCCATCGTGTCTCCC	GCCTGCCATTTATGAGATGTACTGT
Scf_001:5,981,300–5,981,749	GCAAGACTGGCGACAGCATC	AAGACCACGACCGCAGAAATC
scf_003:217,950–218,349	CTGCGAAGAGGAATCGTGGGA	GGACACCTCCAAATTCCTCACTT
Scf_003:2,414,750–2,415,099	GACGACGCCAGGACAAACC	CCTTGGTAGTGATTGACTCGCAGAA
Scf_002:1,616,850–1,617,199	CCCCGTGACTGCTGGGAAAC	CGTGAGGCGTGGGAGAAAGGAA
Scf_002:2,083,850–2,084,199	AATGGCACAGAACGTCGAAACG	CGGCTGGTGGATGGTCAAGT
MAA_09983	AGGCCTTACGATGTACCGTC	ATCATACATAGATCATTCCGCC
MAA_03501	CCCTCATCCATCGTTCTGGTCT	GGCCAACTTGGTCTCGACGCG
MAA_06876	TCTTGTGTATCAACGGCCGAGAC	AACTGGCTCTGCCTCTGCCTCTG
MAA_05503	AGGGAATGTAGGCTATCTGAGATG	GGGCGGGAAGTTCGATGTGCTGG
MAA_00157	CACCGAGGGGAGCTGGGCAATG	ATGTTGCCCTTGGCACCGACC
Primers were designed for real-time PCR		
MAA_09983	GGTGCAGAGCAGAACTTCATTCC	CTTGAGCCTATCGCCAACAACATA
MAA_03501	ATTCTCCGCTATGAGCGATACGA	CATTCAGGGCTGATAATGACTTCC
MAA_06876	AGCCCTTCAATTATTCAAGCAAG	CCATAGCCCATCCAACATACCAT
MAA_05503	CCGATACACGGGATGGTAGTTGAA	TGTCGCCGATGGTACAATGTTGA
MAA_00157	CCTTCTTTGCTTACGCCATACCTG	AAACGATGATCCGTCGAGCCATT
GADPH	GACTGCCCGCATTGAGAAG	AGATGGAGGAGTTGGTGTG

Restriction sites are in italic

<sup>a</sup> Letters in the parentheses refer to primer positions in Fig. 1a, b

inserted into the corresponding sites of the binary vector pDht-SK-ben to produce the binary vector pben-DIM-2 (Fig. 1b). The mutants (deletions of *MrRID*, *MrDIM-2*, and *RID/DIM-2*) were constructed by means of *Agrobacterium*-mediated fungal transformation (ATMT) and replacements by homologous recombination as previously described (Duan et al. 2009).

The complementation vector Com-pben-RID was constructed using the entire *MrRID* gene plus 1.3 and 0.2 kb of the upstream and downstream sequences, respectively (Fig. 1a). The DNA was amplified from WT genomic DNA with primers i and j (Table 1). Then, the products were digested with *Pst*I (TaKaRa, Dalian, China) and inserted into the corresponding sites of the binary vector pDht-SK-ben

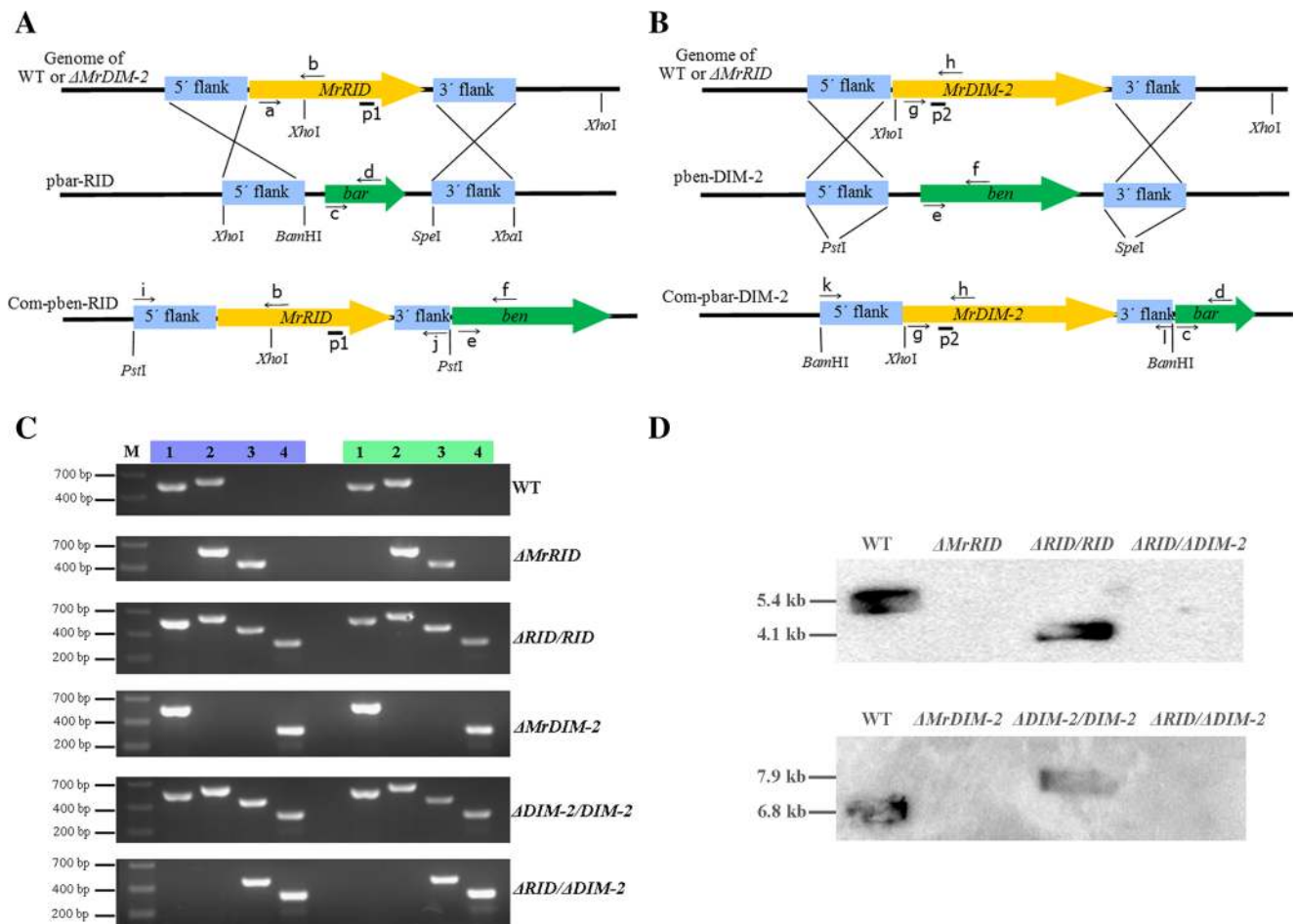


**Fig. 1** Deletion of genes encoding DNMTases in *Metarhizium robertsii*. **a** The disruption and complementation plasmids of *MrRID*. **b** The disruption and complementation plasmids of *MrDIM-2*. **c** Confirmation by PCR shows the disruption of the genes of the mutants. Blue, genomic DNA; light green, cDNA; M, marker; 1, PCR conducted with the primers a and b; 2, PCR conducted with the primers g and h; 3, PCR conducted

with the primers c and d; 4, PCR conducted with the primers e and f; 5, PCR conducted with primers for the glyceraldehyde 3-phosphate dehydrogenase (GAPDH) gene as an internal control for each sample. **d** Southern blotting hybridization with amplified probes with *MrRID* (p1) and *MrDIM-2* (p2) ORF fragments, respectively. Further information on primers can be found in Table 1

(Fig. 1a). The complementation vector Com-pbar-DIM-2 was constructed using the entire *MrDIM-2* gene plus 0.9 and 0.2 kb of the upstream and downstream sequences, respectively (Fig. 1b). The DNA was amplified from WT genomic DNA with primers k and l (Table 1). Then, the products were digested with *Bam*HI (TaKaRa, Dalian, China) and inserted into the corresponding sites of the binary vector pDht-SK-bar (Fig. 1b). The plasmids Com-pben-RID and Com-pbar-DIM-2 were mobilized into AGL-1 and then transformed into different mutants (with deletions of *MrRID* or *MrDIM-2*). All the primers used are listed in Table 1.

### Confirmation of mutants

Single conidia from the gene deletion mutants were isolated by streaking individual colonies on selection plates and confirmed with PCR and reverse transcription PCR (RT-PCR). The genomic DNA was extracted with a Genomic DNA

Extraction Kit (Qiagen, Hilden, Germany). Total RNA was extracted using TRIzol Reagent (Invitrogen, Carlsbad, CA, USA), and first-strand cDNA was synthesized using a PrimeScript™ II 1st Strand cDNA Synthesis Kit (TaKaRa) according to the manufacturer's instructions. The glyceraldehyde 3-phosphate dehydrogenase (GAPDH) gene (MAA\_07675) was used as an internal control. All the primers used are listed in Table 1. For Southern blotting, 30  $\mu$ g samples of genomic DNA extracted from the PDA colonies of WT and each mutant were digested with *Xho*I, separated by electrophoresis in 0.7% agarose gel, and then transferred to Hybond-N<sup>+</sup> membrane (Amersham, Piscataway, USA). The *MrRID* and *MrDIM-2* ORF fragments used as probes were, respectively, labelled with the PCR DIG Labelling Mix Kit (Roche, Penzberg, Germany). Probe preparation, membrane hybridization, and visualization were according to the manufacturer's instructions (DIG High Prime DNA Labelling and Detection Starter Kit II, Roche).

## BS-PCR for selected segments in different mutants

Ten methylated regions, based on genome-wide DNA methylation in *M. robertsii*, deposited in the NCBI GEO database with the accession number GSE78019, were randomly selected, following the categories of high (>66%), medium, and low (<33%) methylated patterns, to examine the methylation changes in different mutants. BS-PCR was performed according to our earlier reports (Wang et al. 2015). One-hundred-microliter aliquots of a conidial suspension from either WT or mutant colonies were spread on PDA plates and incubated in the dark at 28 °C for 12 days. DNAs from these cultures, including both mycelium and conidia, of different strains were used for BS-PCR, and DNA samples per strain were extracted from three independent culture experiments. DNA from these cultures of the different strains was used for BS-PCR. Briefly, DNA (1 µg) was bisulfite converted as previously described (Espada et al. 2014). Two-hundred nanograms of bisulfite-converted DNA was PCR-amplified, and the purified amplicons were cloned into a pMD18-T vector (TaKaRa) and sequenced. An average of 15 clones were randomly chosen to sequence for each segment. All experiments were performed in triplicate. All the primers used are listed in Table 1.

## Phenotypic assays

**Vegetative growth.** PDA plates were spotted in the center with aliquots of conidia harvested from WT and mutant cultures growing on PDA plates. The radial growth (colony diameter) of the vegetative mycelia was measured daily at 28 °C.

**Chemical stress.** Fungal colony disks (5-mm diameter) were cut from cultures of WT and mutants that were grown for 3 days at 28 °C on PDA plates smeared with 100-µl aliquots of a conidial suspension to initiate the cultures. The disks were gently placed in the center of (9-cm diameter) PDA plates containing different chemical reagents, including osmotic (0.5 M NaCl), oxidative (2 mM H<sub>2</sub>O<sub>2</sub>), cell wall (3 mg/ml<sup>-1</sup> Congo red and 2.5 µg/ml<sup>-1</sup> SDS), and fungicidal (2 µg/mL carbendazim) stressors. Radial growth was measured as described earlier, and PDA plates (without any modifications) were used as the control. All experiments were performed in triplicate.

**Conidial yield.** To assess the sporulation capacity of the WT and that of each mutant, 100-µl aliquots of a conidial suspension were spread on PDA plates and incubated for 20 days at 28 °C. From day 3 onwards, colony disks (5-mm diameter) were excised at random from the plates daily. The conidia on each disk were washed off into 2 ml of 0.05% Tween 80 by subjecting each disk to 10 min of supersonic vibration. The concentration of the conidial suspension was determined by counting the conidia using a hemocytometer under a microscope.

**Conidial viability assays.** To assay the fresh conidial germination rates of the strains, 30-µl aliquots of a conidial suspension were spread onto PDA plates (9-cm diameter), followed by incubation at 28 °C for 48 h. From 12 h onwards, the percentage of germinated conidia on each plate was assessed every 4 h by counting the number of germinated conidia that could be seen under the microscope. Three counts were performed for each plate. The morphological development of the germ tubes and the growing hyphae were also examined under a microscope.

**Thermotolerance assays.** Each mutant strain was assayed using a method described elsewhere (Wang et al. 2014). Briefly, 1-ml aliquots of conidial suspensions in 1.5-ml Eppendorf tubes were placed in a water bath at 42 °C for up to 90 min, and then, PDA plates were inoculated with 100 µl of the conidial suspension from each tube. After 24 h of incubation, conidial germination on each plate was observed under the microscope; conidia with visible germ tubes were considered to have germinated.

**UV irradiation assays.** The conidial tolerance of each mutant was assayed using a previous method (Yao et al. 2010). Briefly, 10-µl aliquots of conidia were centrally spotted onto the marked area (10-mm diameter) of glass slides and then exposed to weighted UV-B irradiation at a wavelength of 312 nm (280–320 nm) at gradient doses of 0.1–0.8 J/cm<sup>-2</sup> in a Bio-Sun<sup>++</sup> chamber (Vilber Lourmat, Marne-la-Vallée, France). After exposure, conidial germination on each plate was observed as mentioned above.

All experiments were performed in triplicate, and all data were analyzed as previously reported; the growth inhibition (GI) rate (%) was calculated as  $(C - S)/C \times 100$ , where  $C$  is the growth rate of the control and  $S$  is the growth rate under a given stress (Ying et al. 2013). Residue viability was assessed by determining the percentage of germination, which was calculated using the counts of the number of germinated and ungerminated conidia.

## Bioassays for fungal virulence

WT and *M. robertsii* mutants were bioassayed using *Galleria mellonella* as reported previously (Fang et al. 2009). Conidia were applied topically by immersing larvae for 20 s in an aqueous suspension containing  $1 \times 10^7$  conidia ml<sup>-1</sup>. Each treatment had three replicates with 15 insects in each replicate. The experiments were performed in triplicate. Mortality was recorded every 12 h. The median lethal time (LT<sub>50</sub>) was estimated and compared by performing a Kaplan-Meier analysis using SPSS (version 13.0) (Wang and St Leger 2007).

## BS-PCR and real-time PCR for five selected genes

The genes for tuberin (MAA\_09983) and an autophagy-related protein (MAA\_03501), a DNA repair protein

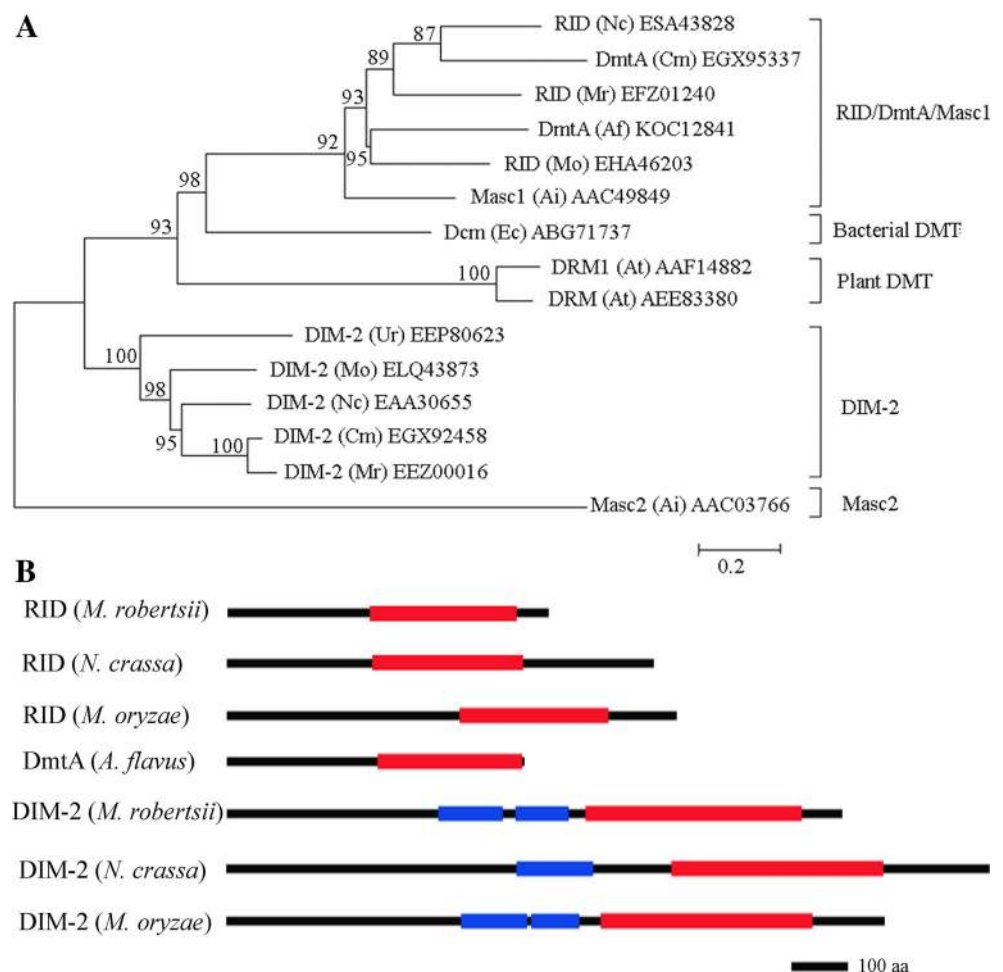
(MAA\_06876), cysteine proteinase (MAA\_05503), and chitinase (MAA\_00157) were selected to examine the effect of DNA methylation on gene transcription. Primers overlapping with the gene promoters (1 kb upstream of the gene-coding regions) and with the gene-coding regions were used for amplification, and BS-PCR was performed as mentioned above (Table 1). Gene expression was detected by RT-PCR, and the specific primers are listed in Table 1; three replicates were performed independently for each gene tested.

## Results

### Identification of genes encoding putative DNMTases

To investigate the function of DNMTases in the entomopathogenic fungus *M. robertsii*, we sought to identify and characterize genes encoding putative DNMTases in the fungal genome. By performing a BLAST search using the amino acid sequences of known DNMTases as queries, we found two genes (*MrRID* and *MrDIM-2*) which encode proteins containing a DNMTase domain (MAA\_03836 and MAA\_04944).

**Fig. 2** DNMTases in diverse organisms. **a** Phylogenetic analysis of DNMTases. The phylogenetic tree was constructed by a neighbor-joining method using the DNMTase domains as representative amino acid sequences of DNMTases. *Af* *Aspergillus flavus*, *Ai* *Ascobolus immersus*, *At* *Arabidopsis thaliana*, *Cm* *Cordyceps militaris*, *Ec* *Escherichia coli*, *Mo* *Magnaporthe oryzae*, *Mr* *Metarhizium robertsii*, *Nc* *Neurospora crassa*, *Ur* *Ucinocarpus reesii*. Bootstrap values are adjacent to each internal node, representing the percentage of 1000 bootstrap replicates. **b** Domain architecture of representative DNMTases. Light green, BAH (bromo-adjacent homology) domain; red, DNMTase domain



Phylogenetic analysis showed that *MrRID* and *MrDIM-2* are closely related to *RID* and *DIM-2* in *N. crassa*. *RID* is responsible for the specificity of DNA methylation and RIP mutation, and *DIM-2* is capable of both de novo and maintenance DNA methylation (Fig. 2a). According to further analysis of the domain architecture, *MrDIM-2*, which is similar to *DIM-2* in *M. oryzae*, is typical of *DIM-2*-type fungal DNMTases that have a long N-terminal extension containing a bromo-adjacent homology (BAH) domain and a C-terminal extension (Fig. 2b) (Jeon et al. 2015).

### Construction and validation of DNMTase mutants

To investigate the role of DNMTases in *M. robertsii*, three targeted insertion mutants were constructed based on the identified sequences. Strains  $\Delta$ *MrRID* and  $\Delta$ *MrDIM-2* were constructed by replacing the coding regions of *MrRID* and *MrDIM-2* with the *bar* and *ben* gene cassettes inserted with flanking fragments of *MrRID* and *MrDim-2* in vectors pbar-RID and pben-DIM-2, respectively (Fig. 1a, b).  $\Delta$ *RID*/ $\Delta$ *DIM-2* was constructed by replacing the coding region of *MrRID* in  $\Delta$ *MrDIM-2* with the *bar* cassette in vector pbar-

RID. Complementation strains ( $\Delta$ RID/RID and  $\Delta$ DIM-2/DIM-2) were obtained by transforming Com-pben-RID and Com-pbar-DIM-2 into strains  $\Delta$ MrRID and  $\Delta$ MrDIM-2, respectively (Fig. 1a, b).

All the mutant strains were confirmed by PCR using genomic DNA as a template. PCR analysis indicated that a partial *MrRID* fragment (528 bp) was present in the WT and  $\Delta$ RID/RID but not in strains  $\Delta$ MrRID and  $\Delta$ RID/ $\Delta$ DIM-2 (Fig. 1c). In addition, a partial *MrDIM-2* fragment (599 bp) was present in the WT and  $\Delta$ DIM-2/DIM-2 but not in strains  $\Delta$ MrDIM-2 and  $\Delta$ RID/ $\Delta$ DIM-2 (Fig. 1c). A 434-bp fragment corresponding to the *bar* gene was present in strains  $\Delta$ MrRID,  $\Delta$ RID/RID,  $\Delta$ DIM-2/DIM-2, and  $\Delta$ RID/ $\Delta$ DIM-2, and a 328-bp fragment corresponding to the *ben* gene was present in strains  $\Delta$ RID/RID,  $\Delta$ MrDIM-2,  $\Delta$ DIM-2/DIM-2, and  $\Delta$ RID/ $\Delta$ DIM-2 (Fig. 1c). RT-PCR was used to further confirm expression of genes in the mutants, using the GAPDH gene (EFY96862) as an internal control for each sample (Fig. 1c). Southern blotting further validated the homologous recombination in the deletion mutants. As expected, the *MrRID* ORF fragment probe detected a 5.4-kb *Xho*I band in the WT and a *Xho*I band of 4.1 kb in the complemented strain  $\Delta$ RID/RID, respectively, but not in strains  $\Delta$ MrRID and  $\Delta$ RID/ $\Delta$ DIM-2 (Fig. 1d). The shorter fragment of 4.1 kb indicates that the complemented strain carries the transformed *MrRID* gene inserted at another site than at the homologous place. However, the probe did not detect any band in strains  $\Delta$ MrRID and  $\Delta$ RID/ $\Delta$ DIM-2, further confirming the loss of the *MrRID* gene in these transformants. The *MrDIM-2* ORF fragment probe detected a 6.8-kb *Xho*I band in the WT and a 7.9-kb *Xho*I band in the complemented  $\Delta$ DIM-2/DIM-2 transformant, respectively (Fig. 1d). The size of the 7.9 kb in the  $\Delta$ DIM-2/DIM-2 transformant suggests

that the transformed *MrDIM-2* DNA inserted at an ectopic place into the genome of mutant  $\Delta$ MrDIM-2. In contrast, no signal was detected in strains  $\Delta$ MrDIM-2 and  $\Delta$ RID/ $\Delta$ DIM-2, confirming that in these strains, the *MrDIM-2* gene was deleted.

### Functional analysis of the role of DNMTases in DNA methylation

To test genetically whether the two putative DNMTase genes are involved in DNA methylation, we checked the DNA methylation status of ten known methylated regions using BS-PCR; 71% ( $\pm 2.4\%$ ), 10% ( $\pm 0.6\%$ ), and 8% ( $\pm 0.4\%$ ) of the <sup>14</sup>C sites remained in  $\Delta$ MrRID,  $\Delta$ MrDIM-2, and  $\Delta$ RID/ $\Delta$ DIM-2, respectively, compared with the WT strain (Figs. 3 and 4). Alignments of the WT strain and the different mutant revealed that 35% ( $\pm 0.3\%$ ) of the remaining <sup>14</sup>C sites in  $\Delta$ MrRID did not overlap with those in the WT strain. In  $\Delta$ RID/ $\Delta$ DIM-2, because of the deletions of *MrRID* in  $\Delta$ MrDIM-2, more than half of the remaining <sup>14</sup>C sites did not overlap with the <sup>14</sup>C sites in  $\Delta$ MrDIM-2. Taken together, MrRID in *M. robertsii* seems to play a role in regulating methylation specificity. Importantly, the <sup>14</sup>C sites that disappeared in  $\Delta$ MrRID were a subset of the missing sites in  $\Delta$ MrDIM-2, which suggests that the methylation of those cytosine sites is accomplished by both MrRID and MrDIM-2 (Figs. 3 and 4). These results are consistent with previous studies in *M. oryzae*, which suggests that DNMTases in different fungi have highly conserved functions (Jeon et al. 2015).

### Phenotypic analyses of the wild type and mutants

The effect of disrupting different DNMTases on vegetative growth was examined by incubating WT and mutant cultures at 28 °C on PDA medium. There was little difference in the

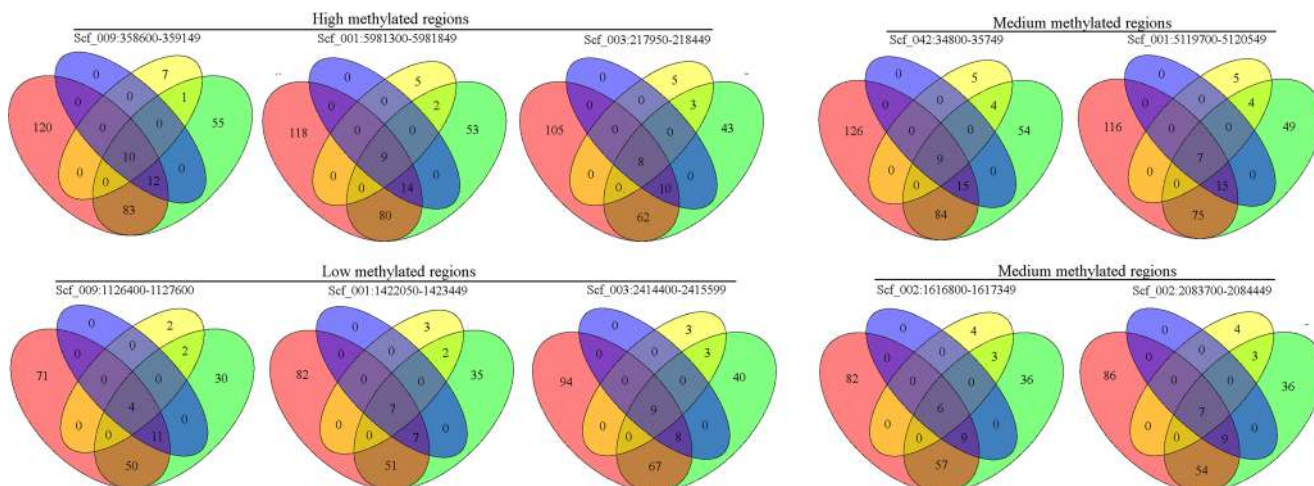
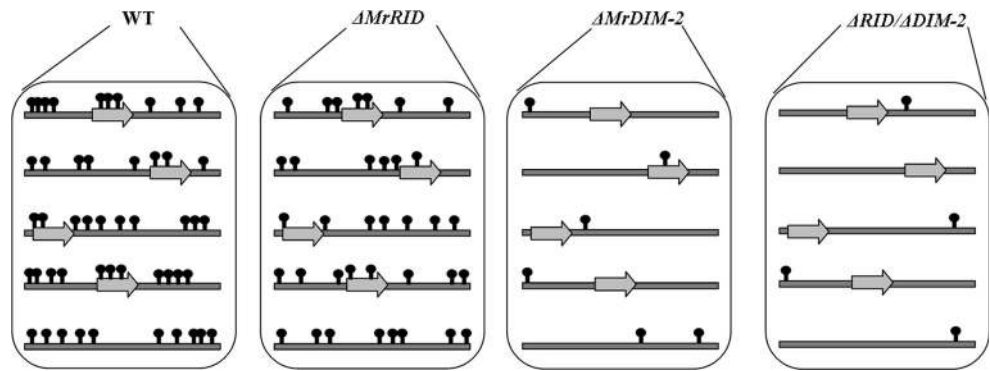


**Fig. 3** Venn diagrams show overlapping and non-overlapping mCs in ten selected regions of the different strains. The red, green, blue, and yellow ellipses refer to the WT,  $\Delta$ MrRID,  $\Delta$ MrDIM-2, and  $\Delta$ RID/ $\Delta$ DIM-2 strains, respectively

**Fig. 4** Model for DNA methylation in the WT,  $\Delta MrRID$ ,  $\Delta MrDIM-2$ , and  $\Delta RID/\Delta DIM-2$  strains. The schematic diagram describes the DNA methylation in and around genes within the nuclear genomes



growth rate between the  $\Delta MrRID$  (2.95 mm/day) and WT strains (3.07 mm/day), while the growth rates of the  $\Delta MrDIM-2$  (1.89 mm/day) and  $\Delta RID/\Delta DIM-2$  (1.81 mm/day) strains were significantly reduced compared with that of the WT strain and the complemented strains (Fig. 5a). Consequently, the number of conidia produced by the colonies differed significantly among these strains (Fig. 5b). Conidiation was more defective in  $\Delta RID/\Delta DIM-2$  and  $\Delta MrDIM-2$  than in  $\Delta MrRID$ ; the conidial yields obtained from these mutant cultures on day 7 were reduced by 57.82, 49.76, and 6.97%, respectively, compared with the yield obtained from the control strains on PDA medium (Fig. 5b). These data indicate that both MrRID and MrDIM-2 affected the normal growth and sporulation of *M. robertsii* but that MrDIM-2 was more influential.

The effects of osmotic (NaCl), oxidative ( $H_2O_2$ ), cell wall (Congo Red and SDS), and fungicidal (carbendazim) stressors were examined on plates containing the indicated chemical reagents with the data presented as the percentage of GI. Contrary to our expectations, the DNMTase mutants showed a similar growth capability against stressful chemicals to that shown by the control strains (Fig. 6a).

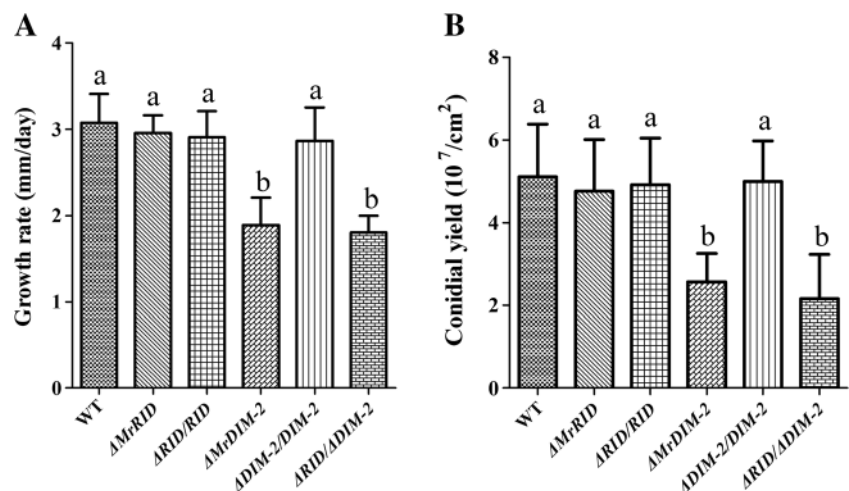
The conidial tolerance of the WT and DNMTase mutants to UV irradiation and heat shock changed dramatically 24 h after

germination. The conidial survival indices were reduced to approximately 42, 17, and 16% for  $\Delta MrRID$ ,  $\Delta MrDIM-2$ , and  $\Delta RID/\Delta DIM-2$ , respectively, while the conidial survival index for the WT strain decreased to 50% after UV-B irradiation. Similar findings were observed for conidial tolerance to the high temperature of 42 °C; 57% of the WT conidia germinated, while only 43, 15, and 14% of the  $\Delta MrRID$ ,  $\Delta MrDIM-2$ , and  $\Delta RID/\Delta DIM-2$  germinated, respectively (Fig. 6b). These data indicated that MrRID and MrDIM-2, and of the two especially MrDIM-2, play important roles in conidial tolerance to both UV irradiation and thermal stress.

#### Virulence of the wild type and mutants

Insect bioassays using the greater wax moth *G. mellonella* were employed to assess the consequences of the loss of *MrRID* and *MrDIM-2* on insect virulence. Insects were infected topically, representing the natural route of infection, and mortality was monitored daily over a 12-day period.  $\Delta MrDIM-2$  and  $\Delta RID/\Delta DIM-2$  insect groups displayed mean lethal times to death ( $LT_{50}$ ) of  $6.5 \pm 0.9$  and  $7.3 \pm 1.2$  days, with a significant ( $P < 0.05$ ) attenuation of virulence, while  $\Delta MrRID$  and the control groups displayed  $LT_{50}$ s of  $4.6 \pm 0.8$  and  $4.4 \pm 0.5$  days,

**Fig. 5** Growth and conidial production of the wild type,  $\Delta MrRID$ ,  $\Delta MrRID/RID$ ,  $\Delta MrDIM-2$ ,  $\Delta MrDIM-2/DIM-2$ , and  $\Delta RID/\Delta DIM-2$ . **a** Growth of WT *M. robertsii* and different mutants. **b** Conidial production was measured for the WT and different mutants. Error bars SD of the mean from three replicate assays





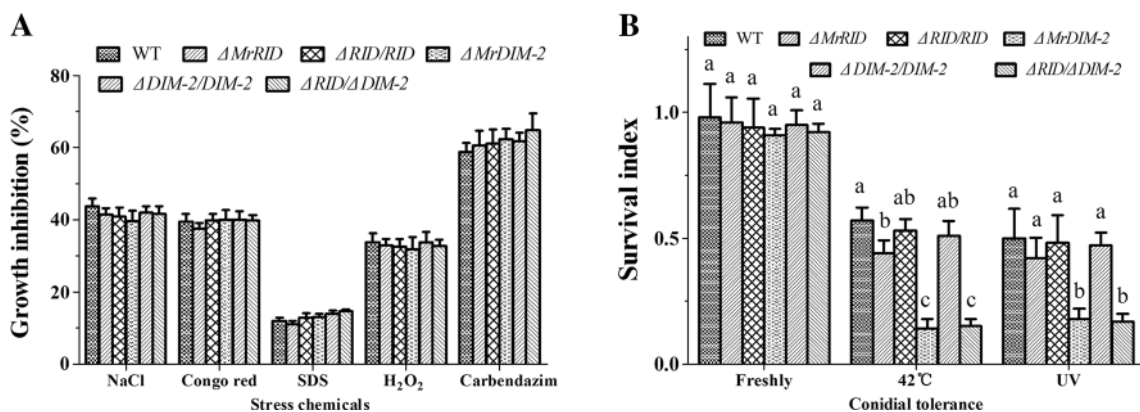


**Fig. 6** Effect of chemical stress reagents on growth and conidial viability of WT *M. robertsii* and different mutants. **a** The GI calculated after incubation of the indicated strains in the presence of different chemical

stress reagents. **b** Conidial viability of WT *M. robertsii* and different mutants under different conditions. Error bars SD of the mean from three replicate assays

respectively. Their  $LT_{50}$ s against *G. mellonella* were decreased by 47.7 and 65.9% for  $\Delta MrDIM-2$  and  $\Delta RID/\Delta DIM-2$ , respectively, but were not significant for  $\Delta MrRID$  ( $P > 0.05$ ) (Fig. 7a). Deletion of *MrDIM-2* delayed not only fungal development and mycosis on an insect cadaver but also sporulation on insect cuticles. Dead larvae were selected and incubated at 28 °C after surface sterilization. Those killed by the  $\Delta MrRID$  and the control strains were mycosed with a heavy layer of conidia, whereas only a fine layer of conidia could be seen on larvae killed by the  $\Delta MrDIM-2$  and  $\Delta RID/\Delta DIM-2$  strains (Fig. 7b). These results indicate that the deletion of *MrDIM-2* impaired fungal virulence and conidiogenesis.

**Effect of DNA methylation on gene transcription**

To clarify the relationship between DNA methylation and the phenotypes mentioned above, some genes (regulation of cellular process, conidia production, response to stress, and virulence) were selected to detect the expression levels. Genes for tuberin (MAA\_09983, regulation of cellular process), an autophagy-related protein (MAA\_03501, conidia production) and a DNA repair protein (MAA\_06876, response to stress), were downregulated in  $\Delta MrDIM-2$  (Goldman et al. 2002; Kikuma et al. 2007; Ying et al. 2013). However, DNA methylation in those gene regions dropped to an average of ~10% compared with the wild type (Fig. S1 in the Supplementary Material). Two important virulence genes, cysteine proteinase

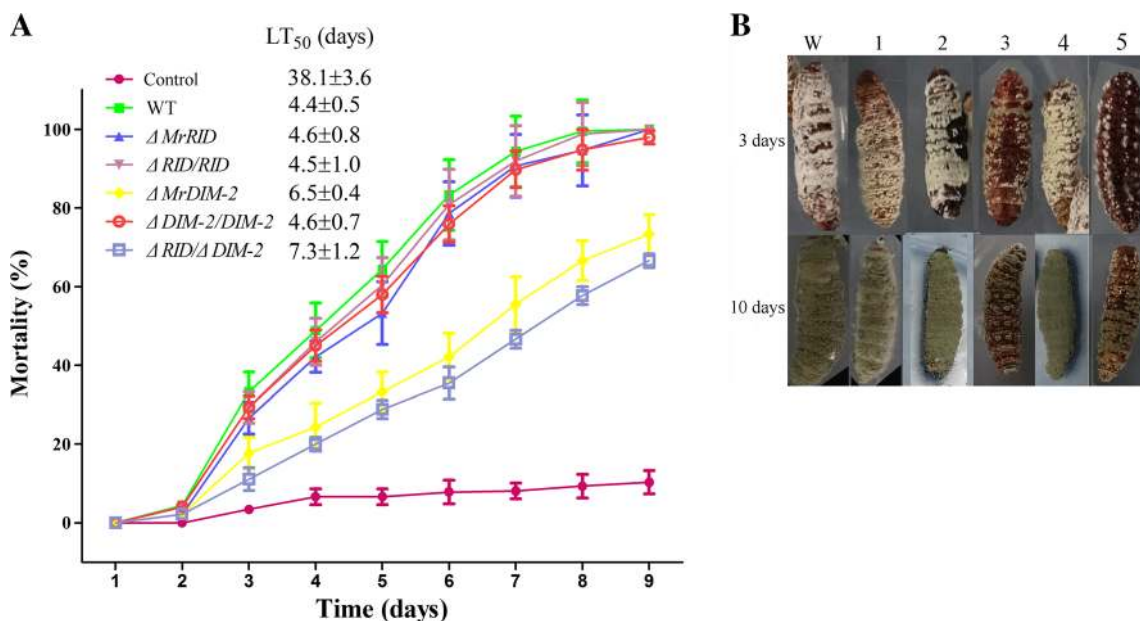


**Fig. 7** Insect bioassays. **a** Mortality of larvae of the greater wax moth *G. mellonella* were treated topically with conidia from the WT and different mutants. Control larvae were treated with sterile distilled  $H_2O$ . **b** Representative images of the insect cadavers treated with the different

strains. W WT, 1  $\Delta MrRID$ , 2  $\Delta MrRID/RID$ , 3  $\Delta MrDIM-2$ , 4  $\Delta MrDIM-2/DIM-2$ , 5  $\Delta RID/\Delta DIM-2$ . Error bars SD of the mean from three replicate assays

(MAA\_05503) and chitinase (MAA\_00157), were selected to detect the relationship between the gene expression levels and DNA methylation patterns (Duan et al. 2013; Niassy et al. 2013). Virulence genes were downregulated in  $\Delta MrDIM-2$ , but in the gene regions, DNA methylation dropped to an average of ~10% compared with the wild type, which is consistent with the results seen in the above genes (Fig. S1 in the Supplementary Material).

## Discussion

DNA methylation is an epigenetic marker that serves as a bridge between genetic components and the environment and plays a vital role in the regulation of gene expression in eukaryotes. DNA methylation was maintained or induced by several DNMTases in different fungal species (Jeon et al. 2015; Kouzminova and Selker 2001; Malagnac et al. 1999). Two putative DNMTases (MrRID and MrDIM-2) were found in *M. robertsii*.

In *N. crassa*, RID is required for RIP, in which most relics of transposons inactivated by RIP are methylated in the genome. RIP introduces C:G-to-T:A transition mutations, creates targets for subsequent DNA methylation, and is always reported to take place during the sexual phase of the life cycle. However, RIP has been reported to occur in at least two asexual fungi (Clutterbuck 2011; Freitag et al. 2002). Genome data demonstrated that *M. robertsii* might have undergone RIP at some stage in its evolution, which suggests that MrRID may be a RIP-defective gene (Gao et al. 2011). Our phylogenetic and functional analyses showed that MrRID is closely related to RID and regulates methylation specificity in the genome. Thus, MrRID likely participated in RIP in *M. robertsii*. The comparison in this study of methylation patterns in the WT strain and different mutants supports that MrRID plays a role in regulating methylation specificity. However, MrRID-dependent mCs showed no sequence preference, which is different from RID in *M. oryzae* (Jeon et al. 2015). Therefore, such specificity is dependent on the chromatin structures, likely modified by the methyltransferase MrRID, without which, new non-specific methylated sites can be produced by MrDIM-2.

The other protein, MrDIM-2, is closely related to DIM-2 from *N. crassa*, which is responsible for all detected cytosine methylation (Kouzminova and Selker 2001). A remaining ~10% of methylated cytosines were found in  $\Delta MrDIM-2$ , which is consistent with previous studies in *M. oryzae*, which suggested that DIM-2 is a major DNMTase in the fungus (Jeon et al. 2015). Approximately 8% of methylated cytosines were found in  $\Delta RID/\Delta DIM-2$ , which shows that the deletion of both MrRID and MrDIM-2 has an additive effect on DNA methylation in *M. robertsii*. In plants, RNA-directed DNA methylation (RdDM) is an important de novo DNA

methylation pathway, in which a 24-nucleotide small interfering RNA (siRNA) guides cytosine methylation (Lewsey et al. 2016; Matzke and Mosher 2014). Previous research has reported that there are many 24-nt siRNAs in *M. robertsii*, suggesting that RdDM may be responsible for DNA methylation in  $\Delta RID/\Delta DIM-2$ , which is a target for future study (Zhou et al. 2012).

The impact of deleting DNMTases on the life cycle of *M. robertsii* was verified by examining the phenotypic changes and stress tolerance of mutants. We observed that the radial growth and conidial production in  $\Delta MrDIM-2$  and  $\Delta RID/\Delta DIM-2$  were more defective when compared to those in the wild type than in  $\Delta MrRID$ , which is similar to observations in *M. oryzae* (Jeon et al. 2015). When comparing the mutant strains to the wild type under UV irradiation or heat, spore viability was noticeably decreased, especially for  $\Delta MrDIM-2$  and  $\Delta RID/\Delta DIM-2$ . This leads to the conclusion that there is a direct link between the loss of DNA methylation and radial growth, conidial production, or viability because MrDIM-2 is responsible for the vast majority of DNA methylation in *M. robertsii*. The genes for tuberin (regulation of cellular process), an autophagy-related protein (conidia production) and a DNA repair protein (response to stress), were downregulated in  $\Delta MrDIM-2$ . However, DNA methylation in those gene regions dropped to an average of ~10% compared with the wild type, which conflicts with the traditional view that DNA methylation inhibits gene expression (Fig. S1 in the Supplementary Material). We speculate that DNA methylation patterns in *M. robertsii* may have unknown roles in gene expression, and more experiments are needed to explore those patterns.

*M. robertsii* is a well-known insect pathogen and is actively being studied as a microbial means of pest control (Gao et al. 2011). In this study, insect bioassays using a topical application of fungal conidia revealed severe attenuation of infection in  $\Delta MrDIM-2$  and  $\Delta RID/\Delta DIM-2$ , along with subsequent poor sporulation in the infected larvae. DNA methylation is correlated with infection-related morphogenesis in *M. oryzae*, which leads to decreased virulence in its mutants (Jeon et al. 2015). However, previous studies could not explain the functional mechanism of DNA methylation in virulence from the perspective of molecular biology. Virulence genes, for cysteine proteinase and chitinase, were downregulated in  $\Delta MrDIM-2$ , but in the gene regions, DNA methylation dropped to an average of ~10% compared with the wild type, which is consistent with the results seen in the above genes (Fig. S1 in the Supplementary Material). Therefore, more work is needed to explore the DNA methylation patterns in *M. robertsii*. There is no difference in virulence between  $\Delta MrRID$  and the WT parent, suggesting that ~25% of the mCs methylated by MrRID do not influence the normal infection of insects.

In conclusion, our data indicate that MrDIM-2 is responsible for almost all DNA methylation, and that MrRID regulates the methylation specificity of the genome in *M. robertsii*, similar to *N. crassa*. DNMTases play an important role in the development, stress tolerance, and virulence of the pathogenic insect fungus *M. robertsii*. Data from this study advance our understanding of the function of DNMTase in entomopathogenic fungi, which should contribute to future epigenetic investigations in fungi.

**Acknowledgement** This work was supported by the National Natural Science Foundation of China (Grant Nos. 31272096, 31471821, and 31572060).

#### Compliance with ethical standards

**Conflict of interest** The authors declare that they have no conflict of interest.

**Human and animal rights** This article does not contain any studies with human participants or animal subjects performed by any of the authors.

## References

- Antequera F, Tamame M, Villanuevaz JR, Santos Q T (1984) DNA methylation in the fungi. *J Biol Chem* 259:8033–8036
- Aramayo R, Selker EU (2013) *Neurospora crassa*, a model system for epigenetics research. *Cold Spring Harb Perspect Biol* 5(10):a017921. doi:10.1101/cshperspect.a017921
- Bidochka MJ, Kamp AM, Lavender TM, Dekoning J, De Croos JN (2001) Habitat association in two genetic groups of the insect-pathogenic fungus *Metarhizium anisopliae*: uncovering cryptic species? *Appl Environ Microbiol* 67(3):1335–1342. doi:10.1128/AEM.67.3.1335-1342
- Cao XF, Jacobsen SE (2002) Role of the *Arabidopsis DRM* methyltransferases in de novo DNA methylation and gene silencing. *Curr Biol* 12(13):1138–1144
- Clutterbuck AJ (2011) Genomic evidence of repeat-induced point mutation (RIP) in filamentous ascomycetes. *Fungal Genet Biol* 48(3):306–326. doi:10.1016/j.fgb.2010.09.002
- Duan Z, Chen Y, Huang W, Shang Y, Chen P, Wang C (2013) Linkage of autophagy to fungal development, lipid storage and virulence in *Metarhizium robertsii*. *Autophagy* 9(4):538–549. doi:10.4161/auto.23575
- Duan Z, Shang Y, Gao Q, Zheng P, Wang C (2009) A phosphoketolase Mpk1 of bacterial origin is adaptively required for full virulence in the insect-pathogenic fungus *Metarhizium anisopliae*. *Environ Microbiol* 11(9):2351–2360. doi:10.1111/j.1462-2920.2009.01961.x
- Espada J, Carrasco E, Calvo MI (2014) Standard DNA methylation analysis in mouse epidermis: bisulfite sequencing, methylation-specific PCR, and 5-methyl-cytosine (5mC) immunological detection. *Methods Mol Biol* 1094:221–231. doi:10.1007/978-1-62703-706-8\_17
- Fang W, Pava-ripoll M, Wang S, St. Leger RJ (2009) Protein kinase A regulates production of virulence determinants by the entomopathogenic fungus, *Metarhizium anisopliae*. *Fungal Genet Biol* 46(3):277–285. doi:10.1016/j.fgb.2008.12.001
- Fang W, St. Leger RJ (2010) RNA binding proteins mediate the ability of a fungus to adapt to the cold. *Environ Microbiol* 12(3):810–820. doi:10.1111/j.1462-2920.2009.02127.x
- Feng SH, Cokus SJ, Zhang XY, Chen PY, Bostick M, Goll MG, Hetzel J, Jain J, Strauss SH, Halpern ME, Ukomadu C, Sadler KC, Pradhan S, Pellegrini M, Jacobsen SE (2010) Conservation and divergence of methylation patterning in plants and animals. *PNAS* 107(19):8689–8694. doi:10.1073/pnas.1002720107
- Foss HM, Roberts CJ, Claeys KM, Selker EU (1993) Abnormal chromosome behavior in *Neurospora* mutants defective in DNA methylation. *Science* 262(5140):1737–1741
- Freitag M, Williams RL, Kothe GO, Selker EU (2002) A cytosine methyltransferase homologue is essential for repeat-induced point mutation in *Neurospora crassa*. *Proc Natl Acad Sci U S A* 99(13):8802–8807. doi:10.1073/pnas.132212899
- Gao Q, Jin K, Ying S-H, Zhang Y, Xiao G, Shang Y, Duan Z, Hu X, Xie XQ, Zhou G, Peng U, Luo Z, Huang W, Wang B, Fang W, Wang S, Zhong Y, Ma LJ, Leger RJS, Zhao GP, Pei Y, Feng MG, Xia Y, Wang C (2011) Genome sequencing and comparative transcriptomics of the model entomopathogenic fungi *Metarhizium anisopliae* and *M. acridum*. *PLoS Genet* 7(1):e1001264. doi:10.1371/journal.pgen.1001264.g001
- Gao Q, Shang Y, Huang W, Wang C (2013) Glycerol-3-phosphate acyltransferase contributes to triacylglycerol biosynthesis, lipid droplet formation, and host invasion in *Metarhizium robertsii*. *Appl Environ Microbiol* 79(24):7646–7653
- Goldman GH, McGuire SL, Harris SD (2002) The DNA damage response in filamentous fungi. *Fungal Genet Biol* 35(3):183–195. doi:10.1006/fgbi.2002.1344
- Jeon J, Choi J, Lee G-W, Park S-Y, Huh A, Dean RA, Lee Y-H (2015) Genome-wide profiling of DNA methylation provides insights into epigenetic regulation of fungal development in a plant pathogenic fungus, *Magnaporthe oryzae*. *Sci Rep* 5:8567. doi:10.1038/srep08567
- Jurkowski TP, Jeltsch A (2011) On the evolutionary origin of eukaryotic DNA methyltransferases and Dnmt2. *PLoS One* 6(11):e28104. doi:10.1371/journal.pone.0028104.g001
- Kikuma T, Arioka M, Kitamoto K (2007) Autophagy during conidiation and conidial germination in filamentous fungi. *Autophagy* 3(2):128–129
- Kouzminova E, Selker EU (2001) *dim-2* encodes a DNA methyltransferase responsible for all known cytosine methylation in *Neurospora*. *EMBO J* 20(15):4309–4323
- Law JA, Jacobsen SE (2010) Establishing, maintaining and modifying DNA methylation patterns in plants and animals. *Nat Rev Genet* 11(3):204–220. doi:10.1038/nrg2719
- Lewsey MG, Hardcastle TJ, Melnyk CW, Molnar A, Valli A, Urlich MA, Nery JR, Baulcombe DC, Ecker JR (2016) Mobile small RNAs regulate genome-wide DNA methylation. *PNAS* 113(6):E801–E810. doi:10.1073/pnas.1515072113
- Li E (2002) Chromatin modification and epigenetic reprogramming in mammalian development. *Nat Rev Genet* 3(9):662–673. doi:10.1038/nrg887
- Liu SY, Lin JQ, Wu HL, Wang CC, Huang SJ, Luo YF, Sun JH, Zhou JX, Yan SJ, He JG, Wang J, He ZM (2012) Bisulfite sequencing reveals that *Aspergillus flavus* holds a hollow in DNA methylation. *PLoS One* 7(1):e30349. doi:10.1371/journal.pone.0030349
- Malagnac F, Grégoire A, Goyon C, Rossignol J-L, Faugeron G (1999) *Mase2*, a gene from *Ascobolus* encoding a protein with a DNA-methyltransferase activity in vitro, is dispensable for in vivo methylation. *Mol Microbiol* 31(1):331–338
- Martienssen RA, Colot V (2001) DNA methylation and epigenetic inheritance in plants and filamentous fungi. *Science* 293(5532):1070–1074. doi:10.1126/science.293.5532.1070

- Matzke MA, Mosher RA (2014) RNA-directed DNA methylation: an epigenetic pathway of increasing complexity. *Nat Rev Genet* 15(6):394–408. doi:10.1038/nrg3683
- Mishra PK, Baum M, Carbon J (2011) DNA methylation regulates phenotype-dependent transcriptional activity in *Candida albicans*. *PNAS* 108(29):11965–11970. doi:10.1073/pnas.1109631108
- Nanty L, Carbajosa G, Heap GA, Ratnieks F, van Heel DA, Down TA, Rakyan VK (2011) Comparative methylomics reveals gene-body H3K36me3 in *Drosophila* predicts DNA methylation and CpG landscapes in other invertebrates. *Genome Res* 21(11):1841–1850. doi:10.1101/gr.121640.111
- Niassy S, Subramanian S, Ekesi S, Bargul JL, Villinger J, Maniania NK (2013) Use of *Metarhizium anisopliae* chitinase genes for genotyping and virulence characterization. *Biomed Res Int* doi:10.1155/2013/465213
- Roberts DW, Leger RJS (2004) *Metarhizium* spp., cosmopolitan insect-pathogenic fungi: mycological aspects. *Adv Appl Microbiol* 54:1–70
- Selker EU, Stevens JN (1987) Signal for DNA methylation associated with tandem duplication in *Neurospora crassa*. *Mol Cell Biol* 7(3):1032–1038
- Selker EU, Tountas NA, Cross SH, Margolin BS, Murphy JG, Bird AP, Freitag M (2003) The methylated component of the *Neurospora crassa* genome. *Nature* 422:893–897
- Shock LS, Thakkar PV, Peterson EJ, Moran RG, Taylor SM (2011) DNA methyltransferase 1, cytosine methylation, and cytosine hydroxymethylation in mammalian mitochondria. *Proc Natl Acad Sci U S A* 108(9):3630–3635
- Suzuki MM, Bird A (2008) DNA methylation landscapes: provocative insights from epigenomics. *Nat Rev Genet* 9(6):465–476. doi:10.1038/Nrg2341
- Selker UE (1997) Epigenetic phenomena in filamentous fungi useful paradigms or repeat-induced confusion? *Trends Genet* 13(8):296–301
- Wang C, St. Leger RJ (2007) A scorpion neurotoxin increases the potency of a fungal insecticide. *Nat Biotechnol* 25(12):1455–1456. doi:10.1038/nbt1357
- Wang C, St. Leger RJ (2014) Genomics of entomopathogenic fungi. In: Martin F (ed) *The ecological genomics of fungi*. Hoboken, NJ, pp 243–260
- Wang YL, Wang ZX, Liu C, Wang SB, Huang B (2015) Genome-wide analysis of DNA methylation in the sexual stage of the insect pathogenic fungus *Cordyceps militaris*. *Fungal Biol* 119(12):1246–1254. doi:10.1016/j.funbio.2015.08.017
- Wang ZX, Zhou XZ, Meng HM, Liu YJ, Zhou Q, Huang B (2014) Comparative transcriptomic analysis of the heat stress response in the filamentous fungus *Metarhizium anisopliae* using RNA-Seq. *Appl Microbiol Biotechnol* 98(12):5589–5597. doi:10.1007/s00253-014-5763-y
- Yao SL, Ying SH, Feng MG, Hatting JL (2010) In vitro and in vivo responses of fungal biocontrol agents to gradient doses of UV-B and UV-A irradiation. *BioControl* 55(3):413–422. doi:10.1007/s10526-009-9265-2
- Ying SH, Feng MG, Keyhani NO (2013) A carbon responsive G-protein coupled receptor modulates broad developmental and genetic networks in the entomopathogenic fungus, *Beauveria bassiana*. *Environ Microbiol* 15(11):2902–2921. doi:10.1111/1462-2920.12169
- Zemach A, McDaniel IE, Silva P, Zilberman D (2010) Genome-wide evolutionary analysis of eukaryotic DNA methylation. *Science* 328(5980):916–919. doi:10.1126/science.1186366
- Zhou Q, Wang Z, Zhang J, Meng H, Huang B (2012) Genome-wide identification and profiling of microRNA-like RNAs from *Metarhizium anisopliae* during development. *Fungal Biol* 116(11):1156–1162. doi:10.1016/j.funbio.2012.09.001